Biosensors and Bioelectronics 24 (2009) 1751–1756

Contents lists available at ScienceDirect

Biosensors and Bioelectronics

journal homepage: www.elsevier.com/locate/bios

Low potential detection of glutamate based on the electrocatalytic oxidation of NADH at thionine/single-walled carbon nanotubes composite modified electrode

Ling Meng[a], Ping Wu[a], Guoxiang Chen[b,*], Chenxin Cai[a,*], Yongming Sun[c], Zhenhong Yuan[c]

[a] Jiangsu Key Laboratory of Biofunctional Materials, College of Chemistry and Environmental Science, Nanjing Normal University, 122 Ninghai Road, Nanjing 210097, PR China
[b] College of Life Science, Nanjing Normal University, Nanjing 210097, PR China
[c] Biomass Energy Center, Guangzhou Institute of Energy Conversion, Chinese Academy of Sciences, Guangzhou 510640, PR China

ARTICLE INFO

Article history:
Received 27 June 2008
Received in revised form 1 September 2008
Accepted 4 September 2008
Available online 11 September 2008

Keywords:
Biosensor
Dehydrogenase
Coenzyme
Glutamate
Carbon nanotubes

ABSTRACT

A glutamate biosensor based on the electrocatalytic oxidation of reduced nicotinamide adenine dinucleotide (NADH), which was generated by the enzymatic reaction, was developed via employing a single-walled carbon nanotubes/thionine (Th–SWNTs) nanocomposite as a mediator and an enzyme immobilization matrix. The biosensor, which was fabricated by immobilizing glutamate dehydrogenase (GlDH) on the surface of Th–SWNTs, exhibited a rapid response (ca. 5 s), a low detection limit (0.1 μM), a wide and useful linear range (0.5–400 μM), high sensitivity (137.3 ± 15.7) μA mM^{-1} cm^{-2}, higher biological affinity, as well as good stability and repeatability. In addition, the common interfering species, such as ascorbic acid, uric acid, and 4-acetamidophenol, did not cause any interference due to the use of a low operating potential (190 mV vs. NHE). The biosensor can be used to quantify the concentration of glutamate in the physiological level. The Th–SWNTs system represents a simple and effective approach to the integration of dehydrogenase and electrodes, which can provide analytical access to a large group of enzymes for wide range of bioelectrochemical applications including biosensors and biofuel cells.

1. Introduction

L-Glutamate, one of the main excitatory neurotransmitters in the central nervous system and neuronal pathways in the brain, plays a major role in various neural functions, and relates to various neurological disorders, as well as to memory and learning processes (Johnston and Rogers, 1998; Smythies, 1999). It has widespread use in food as a flavor enhancing food additive. Therefore, its determination is of interest to both the biological science and food industries.

Much effort has been focused on developing suitable methods for precisely monitoring the glutamate level in its biological environment. Those approaches involve chromatographic techniques (Piepponen and Skujins, 2001), capillary biosensors (Olson Cosford and Kuhr, 1996), chemiluminescence (Blankenstein et al., 1993), capillary electrophoresis (Lada et al., 1998), *etc*. All those methods, however, are considered to be time-consuming and laborious, and require sophisticated and expensive instruments.

More recently, several amperometric biosensors for glutamate monitoring have been reported. Those biosensors are usually based on the glutamate oxidase (GlOx) (Mikeladze et al., 2002; Schuvailo et al., 2006), or the glutamate dehydrogenase (GlDH) (Chakraborty and Raj, 2007; Tang et al., 2007a,b). Basu et al. developed a glutamate biosensor based on co-immobilized GlOx and GlDH on the polycarbonate membrane by the cross-linking procedures (Basu et al., 2006). The GlOx catalyzes the oxidation of glutamate to 2-oxoglutarate in the presence of oxygen, producing H_2O_2 simultaneously. Quantification of glutamate is achieved via electrochemical oxidation of the liberated H_2O_2. However, the oxidation of H_2O_2 usually requires a relatively high positive potential (usually over +0.84 V vs. NHE). Many other electroactive species usually coexisting in the biological fluids can also be oxidized at the high potential and their electrochemical signals thus severely affect the selectivity of the biosensors. Therefore, interference elimination represents a main task to be solved for this type of biosensors. The interference can be partially overcome by coating the biosensor with a membrane impermeable to interferents (Yao et al., 1995), or oxidizing the interferents before they reach the biosensor (Zilkha et al., 1994). Coating with polymeric films leads to lower signals and longer response time due to the additional diffusion barrier, whereas using electrochemical preoxidation displays a risk of oxidizing the substrate of interest. To eliminate this risk, the oxidation of the interferents can be accomplished by enzymatic preoxida-

* Corresponding authors. Tel.: +86 25 83598970.
E-mail addresses: caichenxiin@njnu.edu.cn, cxcai@njnu.edu.cn (C. Cai).

0956-5663/$ – see front matter © 2008 Elsevier B.V. All rights reserved.
doi:10.1016/j.bios.2008.09.001

tion, which was achieved either by incorporating specific enzymes in the sensor configuration or immobilizing them in reactors, thus complicating the biosensor fabrication procedures.

The GlDH-based biosensors involve the electrochemistry of NAD^+ (NAD^+: the oxidation form of β-nicotinamide adenine dinucleotide). The biosensing of glutamate using GlDH requires highly sensitive NADH transducer because the signal of the biosensor is based on detection of the anodic current of enzymatically generated NADH. The selective detection of glutamate in the presence of other interfering compounds is successful only if NADH can be detected at a lower potential (less than 0.241 V vs. NHE). However, the direct oxidation of NADH at unmodified electrodes is not straightforward and requires high overpotential (usually 0.7–1.0 V) owing to the sluggish electron-transfer kinetics (Deore and Freund, 2005). Bare electrodes very often suffer from fouling by the adsorption of oxidation products. Various methodologies have been developed to enhance the electron-transfer kinetics of the oxidation of NADH (Chen et al., 2004; Wu et al., 2007). A conventional way is to fabricate nanomaterial-based electrodes that can promote the electron-transfer kinetics. In this way, much effort has been devoted to identifying/developing new materials which can effectively overcome the kinetic barriers for the oxidation of NADH and regenerate the enzymatically active NAD^+ (Curulli et al., 2005; Wu et al., 2007). Carbon nanotubes (CNTs) have received considerable attention for this purpose. Many studies have demonstrated that CNTs can be used to fabricate the nanostructured macroscopic electrodes, biosensors, and nanobioelectronic devices due to their nanometer size, lack of toxicity, good electrocatalytic properties, efficient accumulation of biomolecules as well as minimization of surface fouling (Chen et al., 2004; Katz and Willner, 2004).

Although CNTs-based electrodes are known to decrease the overpotential for the oxidation of NADH, the extent of decrease is not sufficient enough for the selective detection of NADH (Musameh et al., 2002). The oxidation of NADH at potential of more than 0.34 V (vs. NHE) often suffers from much interference. Therefore, it is essential to develop an electrode, which can catalyze the oxidation of NADH at less positive potential. Our previous work demonstrated that thionine (Th) and SWNTs could synergistically catalyze the electrochemical oxidation of NADH with an anodic potential of less than 0.24 V (vs. NHE) (Meng et al., 2008). The Th–SWNTs-coated electrode allowed highly sensitive amperometric detection of NADH. These results suggest that Th–SWNTs can be used as a biocompatible platform for development of dehydrogenase-based amperometric biosensors. Here, a glutamate biosensor (GlDH–Th–SWNTs/GC) based on Th–SWNTs and GlDH is developed. The characteristics of the biosensor to the detection of glutamate are presented.

2. Experimental

2.1. Chemicals

Glutamate dehydrogenase (GlDH, from bovine liver, EC 1.4.1.3, lyophilized powder, approx. 25 units mg^{-1} protein), NAD^+ (trihydrate), bovine serum albumin (BSA), glutaraldehyde (25% in water), and L-glutamate (monosodium salt, 99%) were purchased from Sigma. Ascorbic acid (AA), uric acid (UA), 4-acetamidophenol (AP), and Th were obtained from Shanghai Chemical Company (Shanghai, China). These chemicals were used as received. SWNTs (<2-nm in diameter, Shenzhen Nanotech Port, Shenzhen, China) were purified following the reported method (Tohji et al., 1996). All other chemicals were of analytical grade. All solutions were prepared with double-distilled water. 0.1 M of phosphate buffer solution was employed as supporting electrolyte. Solutions of GlDH and NAD^+ were freshly prepared using phosphate buffer solution (pH 8.3) immediately before each experiment.

2.2. Preparation of Th–SWNTs and fabrication of the Th–SWNTs/GC electrode

Th–SWNTs nanocomposite and the Th–SWNTs/GC electrode were fabricated as reported previously (Meng et al., 2008). Briefly, Th–SWNTs were prepared by dispersing 2 mg of purified SWNTs into 1 ml of Th aqueous solution (0.5 mM), and stirring for ca. 20 min. Afterwards, the composites were collected by centrifugation, and thoroughly washed at least thrice with water, and finally dried under vacuum at ambient temperature overnight. The Th–SWNTs/GC electrode was fabricated by casting 2 μl of Th–SWNTs suspension (2 mg ml^{-1} in water) onto the surface of pretreated glassy carbon (GC, 3-mm in diameter) electrode. Before use, the solvent was allowed to be evaporated. The SWNTs/GC electrode was prepared using a similar procedure.

2.3. Immobilization of GlDH

Several parameters were optimized to obtain the best voltammetric response and the high performance of biosensor. Typically, GlDH solution (5 mg ml^{-1} in phosphate buffer solution, pH 8.3) was first mixed with 1% of BSA with a volume ratio of 1 to 1. Then, 5 μl of the mixture was coated on the surface of the Th–SWNTs/GC electrode. To prevent the leakage of the enzyme from the electrode surface, the electrode was cross-linked with 4 μl of 20 mM of glutaraldehyde, which could form covalent bonds with BSA and GlDH, respectively, and hold the GlDH on the electrode surface stably. The excess glutaraldehyde can lead to denaturing of the enzyme. The aim of addition of BSA is to bind with the excess glutaraldehyde and prevent the GlDH from denaturation. The resulting electrode was denoted as GlDH–Th–SWNTs/GC electrode, and stored at 4 °C when it was not in use.

The GlDH–SWNTs/GC and GlDH/GC electrodes were fabricated by the similar procedures.

2.4. Apparatus and procedures

Scanning electron microscopic (SEM) images were obtained using a LEO 1530 VP field-emitting scanning electron microscope (Germany). The UV–vis spectroscopic measurements were performed using a Cary 5000 UV–vis–NIR spectrophotometer (Varian, USA). The samples used for UV–vis measurements were prepared by coating the SWNTs and Th–SWNTs suspension on the surface of quartz slide (qs), respectively. After drying, the resultant SWNTs/qs and Th–SWNTs/qs were used for UV–vis measurements. The UV–vis spectrum of GlDH–Th–SWNTs was recorded by immobilizing GlDH on the surface of Th–SWNTs/qs by a similar manner to that of the GlDH–Th–SWNTs/GC electrode. For comparison, UV–vis spectrum of the GlDH, which was immobilized on the surface of quartz slide (GlDH/qs), was also recorded.

The electrochemical experiments were carried out with a CHI 660B electrochemical workstation (CH Instruments). A two-compartment three-electrode cell with the sample volume of 10 ml was employed. A coiled Pt wire and a saturated calomel electrode (SCE) were used as the counter electrode and the reference electrode, respectively. All values of redox potential reported in this work have been adjusted to those versus the normal hydrogen electrode (NHE). This was completed by adding a constant of 0.2412 V to the potential value versus SCE (Bard and Faulkner, 2001). Amperometric detection was performed under an applied potential of 190 mV. The solution was continuously stirred using a magnetic bar at a speed of 250 rpm. A higher speed leads to increase of the

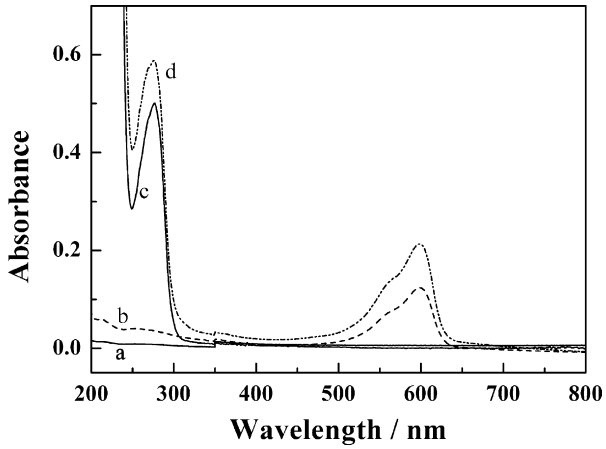

Fig. 1. UV–vis spectra of SWNTs (a), Th–SWNTs (b), GlDH (c), and GlDH-Th–SWNTs (d).

noise while a lower speed results to a longer responsive time. Therefore, it is better to choose an appropriate stirring speed of 250 rpm to obtain a good single-to-noise ratio and a short responsive time. The response current was taken as the change between the steady state and background currents. Buffer was purged with high-purity nitrogen for at least 30 min prior to each experiment and the nitrogen environment was then kept over solution to prevent it from oxygen.

3. Results and discussion

3.1. Characterization

The UV–vis spectrum of the SWNTs exhibits featureless absorption (Fig. 1a), whereas the spectrum of Th–SWNTs displays absorption bands at ca. 600 nm (Fig. 1b), which is the characteristic band of the phenothiazine dye (Li et al., 2004). In the spectrum of Fig. 1b, it can also be observed that a small shoulder peak appears at ca. 560 nm, which results from the absorbance of the polymer of the phenothiazine dye (Du et al., 2007a). These features of Th–SWNTs are almost identical with those of Th in aqueous solution, indicating the adsorption of Th on the SWNTs surface.

The UV–vis spectrum of GlDH–Th–SWNTs is depicted in Fig. 1d. In this spectrum, the adsorption band of Th is identical with that of Fig. 1b. The UV–vis adsorption of GlDH appears at about 275 nm, which is the characteristic peak for polypeptide chains in protein structure (Liu and Cai, 2007). The shape and the position of absorption of GlDH in GlDH–Th–SWNTs composite is almost the same as those for only GlDH immobilized on quartz slide surface (Fig. 1c). These observations suggest that GlDH has been effectively immobilized on Th–SWNTs.

SEM images can provide information of morphologies of Th–SWNTs and the GlDH–Th–SWNTs on the surface of the GC electrode. The image of Th–SWNTs indicates that the composite distributes almost uniformly on the entire surface of the GC electrode exhibiting a special three-dimensional structure with small bundles entangling each other (Fig. 2a). The morphology is different from that reported by Li et al. (2004). They showed that thionine-CNTs composite could not uniformly distribute on the electrode surface representing some agglomerations. The result of Fig. 2a indicates that the Th–SWNTs composite prepared in this work has a good dispersive ability in aqueous solution and can form a well-distributed film on the surface of the electrode. The uniform nanostructure can significantly increase the effective surface of the electrode for loading of biomolecules and accelerating electron-

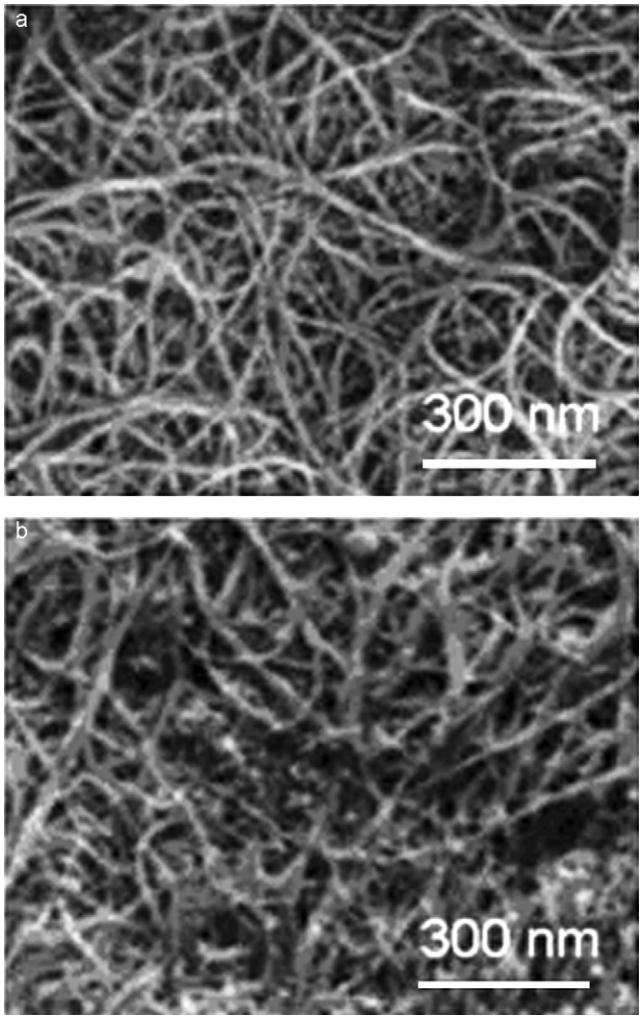

Fig. 2. Typical SEM images of Th–SWNTs (a), and GlDH–Th–SWNTs (b) on GC surface.

transfer. After GlDH was deposited on the surface of Th–SWNTs, some small and uniformly distributed island-like nanostructures appear (Fig. 2b). These nanostructures are the aggregates of the trapped GlDH molecules, indicating that GlDH has been effectively immobilized on the surface of Th–SWNTs. Moreover, the morphology of GlDH–Th–SWNTs on the electrode surface possess the similar three-dimensional structure to that of Th–SWNTs. Such a structure is expected to be very attractive for the detection of substrates because each of the Th–SWNTs is fully and easily accessible to substrates, and thus can be used as an electrochemical sensing unit, yielding a high ratio of signal-to-noise for electrochemical determination.

3.2. Electrochemical oxidation of glutamate at the GlDH–Th–SWNTs/GC electrode

No electrocatalytic response is observed at the GlDH–Th–SWNTs/GC electrode in phosphate buffer solution (0.1 M, pH 8.3) containing 2.5 mM NAD^+ at a scan rate of 2 mV s^{-1} in the potential range of interest (−0.26 to +0.54 V). The cyclic voltammogram of the GlDH–Th–SWNTs/GC electrode is characterized by a pair of well-defined redox peaks with the cathodic (E_{pc}) and anodic (E_{pa}) peak potential of −53 and −26 mV (at 2 mV s^{-1}), respectively (Fig. 3A, curve a). This pair of redox peaks is due to the electrochemical reaction of adsorbed Th. The cathodic and anodic peak

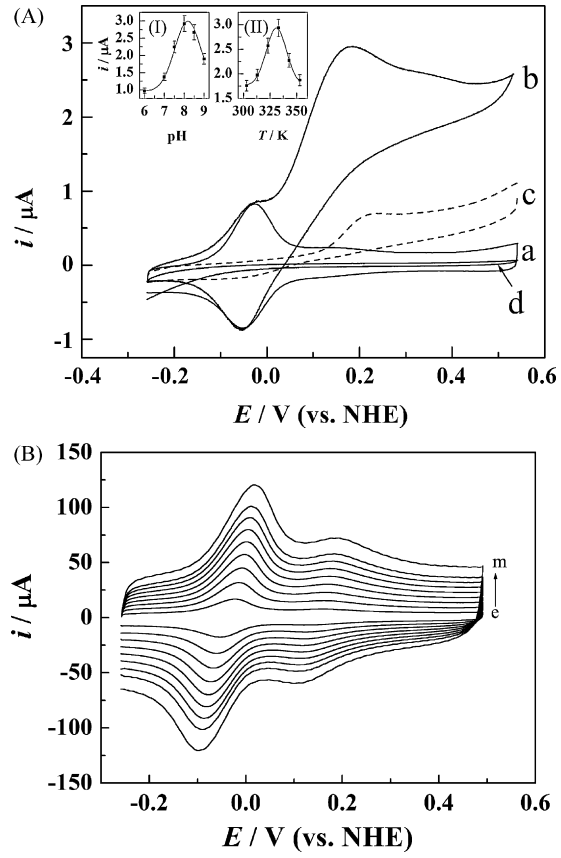

Fig. 3. (A) Voltammetric responses of the GlDH–Th–SWNTs/GC electrode in phosphate buffer solution (0.1 M, pH 8.3) containing 2.5 mM NAD^+ in the absence (curve a) and presence (curve b) of 0.1 mM glutamate. Curves c and d are cyclic voltammograms of the GlDH–SWNTs/GC (c) and GlDH/GC (d) electrode, respectively, in phosphate buffer solution (0.1 M, pH 8.3) containing 2.5 mM of NAD^+ and 0.1 mM of glutamate. The scan rate is 2 mV s^{-1}. The inset (I) and (II) show the dependence of the electrocatalytic current of the electrode on the solution pH (I) and the performing temperature (II), respectively. (B) Cyclic voltammograms of the GlDH–Th–SWNTs/GC electrode in phosphate buffer solution (0.1 M, pH 8.3) at scan rate of (from curves e–m) 100, 200, 300, 400, 500, 600, 700, 800, and 1000 mV s^{-1}.

currents are almost equal at all scan rates (ν) and increase linearly with ν up to at least 1000 mV s^{-1}, indicating that the overall electrochemical process is controlled by a surface reaction. The values of E_{pc} and E_{pa} remain almost invariable when ν is lower than 100 mV s^{-1}. At higher scan rates, E_{pc} and E_{pa} shift to the negative and positive directions, respectively (Fig. 3B). However, $E^{0'}$ (-39 ± 3 mV) is almost independent of ν. The small redox pair at ca. 150 mV (Fig. 3B) is ascribed to the reaction of Th polymer on the surface of SWNTs (Lawrence and Wang, 2006; Meng et al., 2008), indicating that there are some Th polymers on the surface of SWNTs. The conclusion is consistent with that obtained from the UV–vis spectroscopic results. These features are also in good agreement with those obtained at the Th–SWNTs/GC electrode (Meng et al., 2008), indicating that the electrochemical characteristics of Th on the surface of SWNTs remain unchangeable even after GlDH was immobilized. The electrochemical response of the electrode is fairly stable since the shape and size of the redox peaks remain invariant even after the electrode was continuously scanned for a long time (ca. 50 cycles at 2 mV s^{-1}). This characteristic is important when the electrode is used as a biosensor to sense the substrate.

Upon addition of 0.1 mM glutamate, the shape of cyclic voltammogram of the GlDH–Th–SWNTs/GC electrode changes significantly and is characterized by a large anodic peak at ca. 180 mV (Fig. 3A, curve b). The onset potential (at ca. 0 mV) is 180 mV less negative than the oxidation peak actually appears. The GlDH catalyzes, in the presence of NAD^+, the oxidation of glutamate to 2-oxoglutarate, and producing NADH simultaneously. Thus, the anodic peak at curve b of Fig. 3A resulted from the electrocatalytic oxidation of NADH. The anodic peak potential for the NADH oxidation is comparable to that obtained at the chitosan-azure c-CNTs-based electrode (160 mV vs. NHE) (Zhang and Gorski, 2005), and ca. 125, and 455 mV more negative than those obtained at carbon nanofiber (Wu et al., 2007), and peptide nanotube-based electrode (Yemini et al., 2005), respectively. The onset potential is slightly positive than that obtained at meldola's blue-CNTs-based electrode (ca. −60 mV) (Chakraborty and Raj, 2007). The increase of glutamate concentration leads to the enhancement of the anodic current. These characteristics are the typical features of electrocatalytic reactions. Control experiments show that electrocatalytic oxidation of glutamate does not occur at the Th–SWNTs/GC (without GlDH) electrode.

The electrocatalytic activities of the GlDH–SWNTs/GC and GlDH/GC electrodes toward oxidation of glutamate were also recorded, and compared with that of the GlDH–Th–SWNTs/GC electrode. The activity of GlDH/GC electrode is too low to be analyzed quantitatively (Fig. 3A, curve d). The cyclic voltammogram of the GlDH–SWNTs/GC electrode in phosphate buffer solution (0.1 M, pH 8.3) containing 2.5 mM NAD^+ and 0.1 mM glutamate shows an anodic peak at ca. 220 mV (Fig. 3A, curve c). The onset potential is at ca. 110 mV. The peak potential and the onset potential are 40 and 110 mV more positive than those obtained at the GlDH–Th–SWNTs/GC electrode (Fig. 3A, curve b). Moreover, the electrocatalytic current obtained at the GlDH–SWNTs/GC electrode is about 1/4 of that at GlDH–Th–SWNTs/GC electrode (0.50 vs. 2.1 μA. The currents were measured by subtracting the background from the peak current). These results suggest that the electrocatalytic activity of the GlDH–Th–SWNTs/GC electrode is much higher than that of the GlDH–SWNTs/GC electrode. The high activity of the GlDH–Th–SWNTs/GC electrode may come from the synergistic characteristics of Th and SWNTs toward the oxidation of NADH.

The activity of dehydrogenase usually depends on the solution pH, performance temperature, and the concentration of coenzyme. In this work, these conditions were optimized. The response was independently tested thrice for each pH, temperature, and the concentration of NAD^+, and an average value was calculated. The electrocatalytic current increases with the concentration of NAD^+ up to 2.0 mM. It reaches a relatively stable value when the concentration of NAD^+ increases to 2.5 mM, and stays practically constant afterward. The highest electrocatalytic response corresponds to a temperature of ~330 K (~57 °C, the inset (II) of Fig. 3A), and pH 8.3 (the inset (I) of Fig. 3A). The optimal pH is almost identical to that for GlDH in solution (pH 8.25) (Hudson et al., 1993). The optimal temperature obtained in this work is also similar to that obtained by immobilizing GlDH in a carbon paste working electrode (333 K) (Jeffries et al., 1997). Thus, phosphate buffer solution (0.1 M) with pH 8.3, temperature of 330 K (57 °C), and an NAD^+ concentration of 2.5 mM are chosen as the optimal conditions for the GlDH–Th–SWNTs/GC electrode sensing glutamate.

Bovine liver GlDH is a hexameric enzyme containing chemically identical subunits (Cassman and Schachman, 1971). Its activity is affected by a variety of anions and cations. For the cation effects, the Ca^{2+} and Mg^{2+} were reported to affect stability of the enzyme (McCarthy and Tipton, 1984). Zn^{2+} can induce a conformation change and thus causes inhibition of the enzyme (Bell et al., 1987). Lanthanide ions La^{3+} and Eu^{3+} can enhance the activity of the enzyme (Zhuang et al., 2000). However, those results were obtained with GlDH in solution. This work chooses Zn^{2+} and Eu^{3+} as the

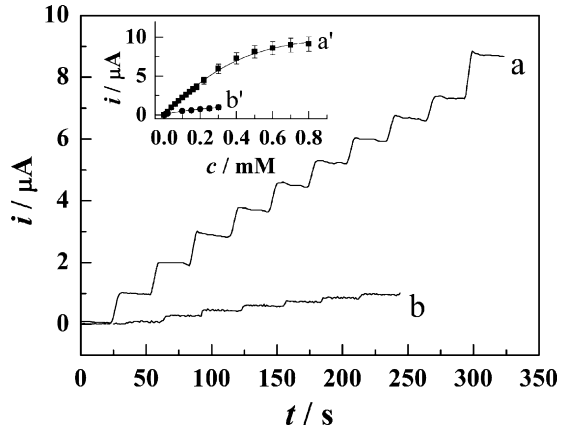

Fig. 4. Successive amperometric responses of the GlDH–Th–SWNTs/GC (a) and GlDH–SWNTs/GC (b) electrode to the glutamate in phosphate buffer solution (0.1 M, pH 8.3) at an applied potential of 190 mV. The each addition of glutamate is 50 μM. The inset shows the dependence of the response of the GlDH–Th–SWNTs/GC (a′) and GlDH–SWNTs/GC (b′) electrode on glutamate concentration under the optimal condition.

models to study the effects of cations on the activity of GlDH immobilized on the surface of Th–SWNTs. The catalytic currents have a clear decrease if Zn^{2+} is added into solution (the results are not shown here), suggesting that Zn^{2+} has a significant inhibitory effect on the activity of the immobilized GlDH. Moreover, the catalytic current further decreases with the increase of the concentration of Zn^{2+}. These features are similar to those reported previously for GlDH in solution (Bell et al., 1987).

The effects of Eu^{3+} on the activity of immobilized GlDH are also studied. Eu^{3+} can slightly enhance the activity of the enzyme since the catalytic currents increase slowly with the concentration of Eu^{3+}. This characteristic is in agreement with that obtained with GlDH in solution (Zhuang et al., 2000).

3.3. Analytical performances of the GlDH–Th–SWNTs/GC electrode

Fig. 4a shows the amperometric response of the GlDH–Th–SWNTs/GC electrode at 190 mV to the successive addition of 50 μM glutamate in solution (pH 8.3). The detection potential, which is chosen from the plateau potential in the hydrodynamic voltammogram (not shown here), is similar to those at GlDH-MWNTs-chitosan-based (140 mV) (Chakraborty and Raj, 2007), and GlDH-Os-gel-HRP-based electrode (240 mV) (Liu et al., 1999). However, it is 250 mV lower than that used for a glutamate biosensor based on self-assembling GlDH on Pt nanoparticles (440 mV) (Tang et al., 2007a). The low detection potential will significantly diminish the influence of those easily oxidizable species. Immediately after the addition of glutamate, the response increases and reaches a steady state within ca. 5 s. The response time is much lower than that obtained with GlOx (20–30 s) (Karyakin et al., 2000), suggesting that the electrode responds rapidly to the change of the substrate concentration. The electrode linearly responds to glutamate at lower concentration and attains saturation level at higher concentration as expected for Michaelis–Menten type enzyme kinetics (the curve (a′) in the inset). The apparent Michaelis–Menten constant (K_{app}^{M}) is estimated to be 1.74 mM from the Lineweaver–Burk plot. The response displays a linear range from 0.5 to 400 μM with a correlation coefficient of 0.996 and a slope of $(18.4 \pm 2.1)\ \mu A\ mM^{-1}$. Therefore, the sensitivity is calculated to be $(137.3 \pm 15.7)\ \mu A\ mM^{-1}\ cm^{-2}$. The apparent surface area of the electrode is estimated using the method reported previously (Du et al., 2007b). The linear range is useful since the normal glutamate concentration in extracellular space is in the range between 1 and 80 μM (Hu et al., 1994), suggesting that the GlDH–Th–SWNTs/GC electrode can be used as a biosensor to sense glutamate in the physiological level. The limit of detection is estimated to be ca. 0.1 μM (at S/N = 3), which is much lower than that obtained at a glutamate microbiosensor based on GlOx (2.5 μM) (Schuvailo et al., 2006). The linear response range is wider than that of 0.2–250 μM reported previously (Tang et al., 2007a). The sensitivity is also much higher than that acquired previously $(0.71 \pm 0.08\ \mu A\ mM^{-1})$ (Chakraborty and Raj, 2007).

Fig. 4b depicts the amperometric responses of the GlDH–SWNTs/GC electrode to the change of concentration of glutamate. The response increases very slowly with the each addition of glutamate due to its lower electrocatalytic activity. The curve (b′) in the inset of Fig. 4 shows that the response is almost independent of glutamate concentration. These results indicate that the GlDH–Th–SWNTs/GC electrode possesses higher biological affinity for glutamate.

Different aspects regarding the characteristics of the GlDH–Th–SWNTs/GC electrode are evaluated. The relative standard deviation (R.S.D.) is ca. 3.2% estimated from the response of five different and freshly prepared electrodes, revealing an acceptable repeatability in the construction of the electrode. The assay precision of the biosensor was examined by five determinations at a glutamate concentration of 0.1 mM. A R.S.D. of ca. 3.8% is obtained. The batch-to-batch repeatability is estimated with the slopes of calibration plots obtained from five independent electrodes. The R.S.D. of these slopes is ca. 4.1%. Also, the stability of the electrode is considered. When the electrode was not in use, it was stored in buffer at 4 °C. Its response to 0.1 mM glutamate was recorded at 1–2 day interval. The response decreases rapidly at the initial few days (~3 days), and afterward the response tends to be practically constant and can still retain ca. 93% of its original response even after 2 weeks' storage. Even after the biosensor has been used continually for 1 week (four measurements a day), its response still remains at ca. 85% of the initial value. These results on the stability can be, in general, advantageously compared with those reported for the CNTs-based biosensors (Chakraborty and Raj, 2007; Tang et al., 2007a). The high stability can be attributed to the capability of the Th–SWNTs composite adsorbing GlDH molecules and retaining their biological activities. This improved stability may also be attributed to the special three-dimensional structure of the GlDH–Th–SWNTs (Fig. 2b), which is beneficial for the substrates getting access to the enzyme molecules. In addition, the fast diffusion of species from nanotubes, and the protection of enzyme by BSA and glutaraldehyde may also contribute to the improvement in stability of the electrode.

In real samples, some co-existing electroactive species, for example, AA, UA, AP, *etc*., might affect the biosensors response. The selectivity and anti-interference advantages of the biosensor are demonstrated in Fig. 5, which compares amperometric responses of three relevant electroactive species (AA, UA, and AP, at a level of 0.1 mM, respectively) and glutamate (also at a level of 0.1 mM). The addition of glutamate results in a well-defined response, however, the successive addition of each interfering species does not bring out discernible current response (Fig. 5). This feature is largely attributed to the low operating potential used in the determination. Thus, highly selective response to glutamate is obtained without the use of perm-selective membrane or enzymatic preoxidation. This is another advantage of the proposed biosensor over those reported previously. These results indicate the suitability of the proposed glutamate biosensor to practical applications.

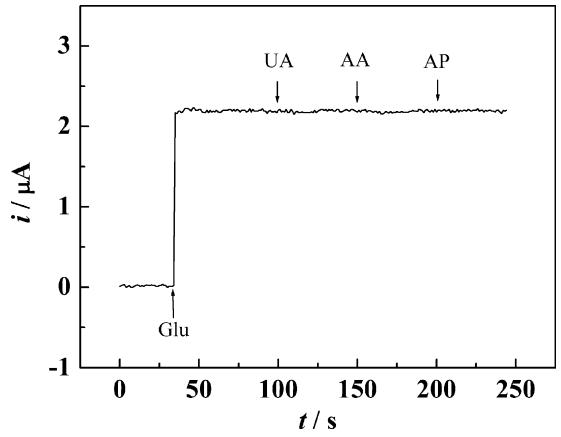

Fig. 5. Amperometric responses of the GlDH–Th–SWNTs/GC electrode upon additions of glutamate (0.1 mM), AA (0.1 mM), UA (0.1 mM), and AP (0.1 mM) in phosphate buffer solution (pH 8.3). The electrode was biased on the potential of 190 mV.

4. Conclusions

A new amperometric glutamate biosensor (GlDH–Th–SWNTs/GC) based on the immobilization of GlDH on the surface of Th–SWNTs composite has been developed. The biosensor exhibited fast response, broad and useful linear range, low detection limit with satisfactory stability, repeatability, and selectivity, and would have potential application in glutamate determination. The fabrication method of the biosensor has many advantages such as ease of fabrication, enhanced electrocatalysis, efficiently preserving the activity of enzyme molecules.

Acknowledgements

This work is supported by the National Natural Science Foundation of China (20673057, 20773067), the Program for New Century Excellent Talents in University (NET-06-0508), and the "863" Project (2007AA05Z154).

References

Bard, A.J., Faulkner, L.R., 2001. Electrochemical Methods, Fundamental and Applications, 2nd ed. John Wiley & Sons, New York.
Bell, E.T., Stilwell, A.M., Bell, J.E., 1987. Biochem. J. 246, 199–203.
Blankenstein, G., Preuschoff, F., Spohn, U., Mohr, K.H., Kula, M.R., 1993. Anal. Chim. Acta 271, 231–237.
Basu, A.K., Chattopadhyay, P., Roychudhuri, U., Chakraborty, R., 2006. Biosens. Bioelectron. 21, 1968–1972.
Cassman, M., Schachman, H.K., 1971. Biochemistry 10, 1015–1024.
Chakraborty, S., Raj, C.R., 2007. Electrochem. Commun. 9, 1323–1330.
Chen, J., Bao, J., Cai, C.X., Lu, T., 2004. Anal. Chim. Acta 516, 29–34.
Olson Cosford, R.J., Kuhr, W.G., 1996. Anal. Chem. 68, 2164–3169.
Curulli, A., Valentini, F., Padeletti, G., Viticoli, M., Caschera, D., Palleschi, G., 2005. Sens. Actuator B: Chem. 111, 441–449.
Deore, B.A., Freund, M.S., 2005. Chem. Mater. 17, 2918–2923.
Du, P., Shi, Y.M., Wu, P., Zhou, Y.M., Cai, C.X., 2007a. Acta Chim. Sinica 65, 1–9.
Du, P., Liu, S., Wu, P., Cai, C.X., 2007b. Electrochim. Acta 52, 6534–6547.
Hu, Y., Mitchell, K.M., Albahadity, F.N., Michaelis, E.K., Wilson, G.S., 1994. Brain Res. 659, 117–125.
Hudson, R.C., Ruttersmith, L.D., Daniel, R.M., 1993. Biochim. Biophys. Acta 1202, 224–250.
Jeffries, C., Pasco, N., Baronian, K., Gorton, L., 1997. Biosens. Bioelectron. 12, 225–232.
Johnston, A.N.B., Rogers, L.J., 1998. Pharmacol. Biochem. Behav. 60, 863–871.
Karyakin, A.A., Karyakina, E.E., Gorton, L., 2000. Anal. Chem. 72, 1720–1723.
Katz, E., Willner, I., 2004. Chem. Phys. Chem. 5, 1084–1104.
Lada, M.W., Vickroy, T.W., Kennedy, R.T., 1998. J. Neurochem. 70, 617–625.
Lawrence, N.S., Wang, J., 2006. Electrochem. Commun. 8, 71–76.
Li, Q., Zhang, J., Yan, H., He, M., Liu, Z., 2004. Carbon 42, 287–291.
Liu, S., Cai, C.X., 2007. J. Electroanal. Chem. 602, 103–114.
Liu, Z., Niwa, O., Horiuchi, T., Kurita, R., Torimitsu, K., 1999. Biosens. Bioelectron. 14, 631–638.
McCarthy, A.D., Tipton, K.F., 1984. Biochem. J. 220, 853–855.
Meng, L., Wu, P., Chen, G., Cai, C.X., 2008. J. Electrochem. Soc. 155, F231–F236.
Mikeladze, E., Collins, A., Sukhacheva, M., Netrusov, A., Csöregi, E., 2002. Electroanalysis 14, 1052–1059.
Musameh, M., Wang, J., Merkoci, A., Lin, Y., 2002. Electrochem. Commun. 4, 743–746.
Piepponen, T.P., Skujins, A., 2001. J. Chromatogr. B: Biomed. Sci. Appl. 757, 277–283.
Schuvailo, O.M., Soldatkin, O.O., Lefebvre, A., Cespuglio, R., Soldatkin, A.P., 2006. Anal. Chim. Acta 573–574, 110–116.
Smythies, J., 1999. Eur. J. Pharmacol. 370, 1–7.
Tang, L., Zhu, Y., Xu, L., Yang, X., Li, C., 2007a. Talanta 73, 438–443.
Tang, L., Zhu, Y., Yang, X., Li, C., 2007b. Anal. Chim. Acta 597, 145–150.
Tohji, K., Goto, T., Takahashi, H., Shinoda, Y., Shimizu, N., Jeyadevan, B., Matsuoka, I., 1996. Nature 383, 679.
Wu, L., Zhang, X., Ju, H., 2007. Anal. Chem. 79, 453–458.
Yao, T., Suzuki, S., Nishino, H., Nakahara, T., 1995. Electroanalysis 7, 1114–1117.
Yemini, M., Reches, M., Gazit, E., Rishpon, J., 2005. Anal. Chem. 77, 5155–5159.
Zhang, M., Gorski, W., 2005. Anal. Chem. 77, 3960–3965.
Zhuang, Q.K., Dai, H.C., Gao, X.X., Xin, W.K., 2000. Bioelectrochemistry 52, 37–41.
Zilkha, E., Koshy, A., Obrenovitch, T.P., Bennetto, H.P., Symon, L., 1994. Anal. Lett. 27, 453–473.